Solid Freeform Fabrication 2019: Proceedings of the 30th Annual International Solid Freeform Fabrication Symposium – An Additive Manufacturing Conference
Reviewed Paper

IN-SITU LAYER-WISE QUALITY MONITORING FOR LASER-BASED ADDITIVE MANUFACTURING USING IMAGE SERIES ANALYSIS

Mehrnaz Noroozi Esfahani[*], Linkan Bian[*†], Wenmeng Tian[*†]

[*]Department of Industrial and Systems Engineering, Mississippi State University, Mississippi State, MS 39762
[†]Center for Advanced Vehicular Systems (CAVS), Mississippi State University, MS 39762

Abstract

Quality assurance has been one of the major challenges in laser-based additive manufacturing (AM) processes. This study proposes a novel process modeling methodology for layer-wise in-situ quality monitoring based on image series analysis. An image-based autoregressive (AR) model has been proposed based on the image registration function between consecutively observed thermal images. Image registration is used to extract melt pool location and orientation change between consecutive images, which contains sensing stability information. Subsequently, a Gaussian process model is used to characterize the spatial correlation within the error matrix. Finally, the extracted features from the aforementioned processes are jointly used for layer-wise quality monitoring. A case study of a thin wall fabrication by a Directed Laser Deposition (DLD) process is used to demonstrate the effectiveness of the proposed methodology.

1. Introduction

Additive Manufacturing (AM) processes add material in layer-by-layer fashion to achieve the final geometry, which enables new design options that cannot be obtained through conventional manufacturing technologies [1]. Nevertheless, quality issues of AM parts are major barriers preventing wider industrial adoption of AM. Due to the existence of defects such as porosity and cracking, the mechanical properties of additively manufactured parts can hardly satisfy the strict requirements of industrial application. AM processes are governed by the process-structure-property (PSP) relationship. Once the PSP relationship is established, the build structure and properties can be predicted. The melt pool images are regarded as a most informative process signature for build structure prediction. In this paper, a novel layer-based quality characterization method is proposed for layer-wise anomaly detection for potential process correction/control actions during the fabrication. Figure 1 shows a schematic plot of a Direct Laser Deposition Process (DLD) fabrication process monitored by a coaxial pyrometer.

The challenges confronting layer-based process anomaly detection are two-fold: 1) there is a huge amount of uncertainty in the relationship between the compositional and process parameters in the basic thermo-mechanical process of metal printing; 2) the advanced sensing technologies provide high volume of noisy thermal history data that represent complex spatio-temporal relationship. To model correlation between thermal history and microstructure properties, finite element methods (FEMs) have been widely used. The thermal behavior and temperature distribution and their effects on the stress, formation, and hardness of parts along with phase transformation during the AM process have been thoroughly studied in the literature [2, 3].

However, there are some challenges in the FEM based approaches that hinder their application in online prediction [4]: 1) high computational cost required, making it extremely time consuming to implement in real time; 2) their high dependency on part geometry which makes it almost impossible to generalize between different designs; and 3) the deterministic nature of FEM related approaches, making it difficult to incorporate all sources of process uncertainty in the modeling for anomaly detection.

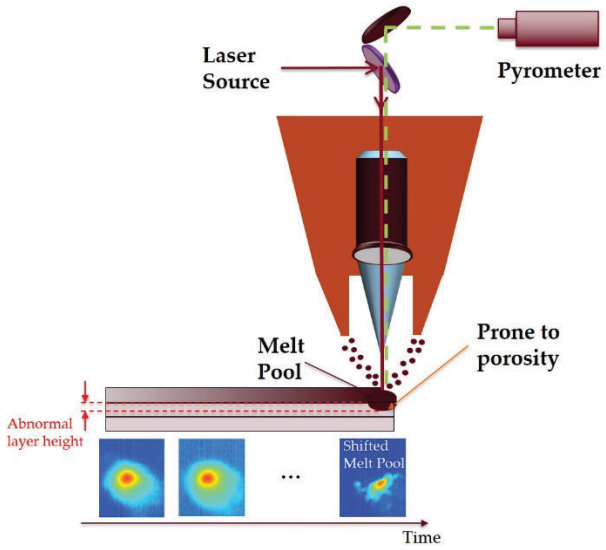

Figure 1: DLD process monitored by a co-axial pyrometer

The advancement in sensing technologies has enabled real-time monitoring of thermal history for anomaly detection via infrared thermography, generating thermal imaging data streams with extremely large volume and complex structure. Although existing data-driven methods consider robust statistical methods to identify anomalies from thermal image [5-6], local features for prediction purposes are used in most of the existing work and, consequently, they cannot be directly utilized to distinguish the profile of an entire deposited layer. This being the case, layer-wise process signature has received the attention of the AM community. Liu et al. [7] has modeled layer-wise spatial porosity evolution based on X-ray computed tomography (XCT), which is an expensive and time-consuming process. Furthermore, optical imaging systems have been used in laser powder bed fusion systems for layer-wise monitoring [8]. Moreover, layer-wise anomaly detection based on thermal history has also been proposed which incorporates a tensor-based dimension reduction and a convex hull based variability characterization approach [9].

In this paper, a novel data-driven methodology is proposed to extract layer-wise process signatures from real-time thermal history for direct laser deposition (DLD) processes. AM process knowledge is leveraged to develop the novel approach. Therefore, the major assumption of the proposed methodology is that a stable thermal history leads to homogenous microstructure and thus porosity-free deposited layers. As illustrated in Figure 1, when there is a layer height anomaly occurring in the process, the observed melt pool in the thermal image will shift in both shape and location. Based on this observation, process features can be proposed to quantify the change in the thermal image series obtained from fabricating one layer. Therefore, process features can be extracted from two sources in the thermal image series, 1) image registration information; and 2)

first order difference of the registered thermal images. Subsequently, the extracted features are used for anomaly detection for each deposited layer in the DLD process.

The rest of the paper is structured as follows. Section 2 provides the proposed framework for layer-wise process feature extraction and anomaly detection, while Section 3 uses a case study of fabricating a thin wall using a DLD process to validate the proposed methodology. Finally, Section 4 summarizes the conclusion and potential future research directions.

2. Methodology

2.1. Data Description and Challenges

Thermal history indicates the thermal response during AM fabrication as a function of time, which is represented by an image series (video) captured by a pyrometer camera during the build. In the thermal images, a region of superheated molten metal is defined as the melt pool [10]. As a key signature of the fabrication process, the melt pool initiates the solidification process in AM and thus is informative to predict part porosity information. Each melt pool image contains location-based temperatures, and each layer can be considered as a series of images. Most of the currently available approaches use individual melt pool image for anomaly detection at the specific location where the melt pool is observed during the fabrication. However, plenty of spatio-temporal correlation information presents in the image series which can be used for anomaly detection and quality prediction. The monitoring of layer-wise thermal history is challenging due to 1) complex spatio-temporal correlation, 2) high dimensionality of thermal images, 3) discrete data sampling, and 4) unreliable and missing data.

2.2. Thermal Image Series Analysis

In this subsection, the proposed framework for modeling the thermal image series collected from fabricating one layer is briefly described. A thermal image time series collected from fabricating one layer can be modeled as an image-based autoregressive model,

$$X_{t+1} = f_{t+1}(X_t, \mathbf{\Omega}_t) + \varepsilon_{t+1} \quad (1)$$

where X_t denotes the thermal image with a dimension of $I \times J$ collected at time stamp t ($t = 1,2, \dots, T_l - 1$) in which T_l denotes the number of images collected when fabricating the l-th layer. It is worth noting that T_l is possible to vary for different layers; f_{t+1} is an image registration function between X_t and X_{t+1} in one layer characterized by a 3×3 transformation matrix $\mathbf{\Omega}_t$. ε_{t+1} denotes an error matrix (with a dimension of $I \times J$) representing the piece of information that cannot be explained by the registration operation. A Gaussian process model is used here to characterize the error term ε_{t+1}, and the detailed information is included in subsection 2.2.2. Figure 2 shows the consecutive melt pool images as an image series, and briefly illustrates the proposed formulation in Equation (1).

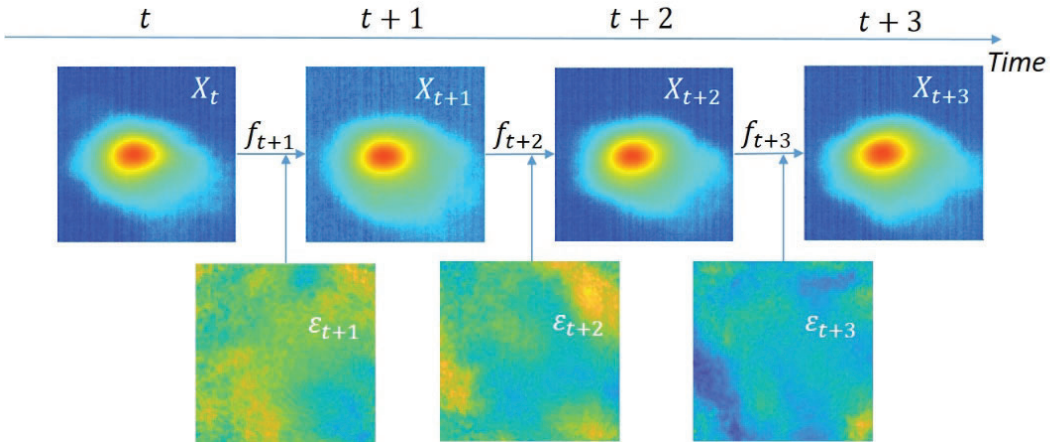

Figure 2: Layer-wise thermal image series formulation

2.2.1 Image Registration

Image registration is a widely used image processing technique that reveals some hidden relationship between the input and the reference images in applications such as health care industry [11], computer vision for target localization, automatic quality control, motion tracking, and cartography for map updating. A registration function is usually in the form of a coordinate transformation matrix.

In this paper, image registration is used to project X_t to X_{t+1} $(t = 1,2, \dots, T_l - 1)$ for the best alignment, and each registration function f_t can involve operations including translation and rotation. More specifically, translation describes the shift magnitude in a 2D coordinate system between X_t and X_{t+1}; rotation describes the orientation difference between X_t and X_{t+1}. The image registration algorithm is performed in an iterative procedure to optimize a pre-defined similarity metric (such as mean square error). The image operations iteratively modify X_t to best match X_{t+1} for a smaller mean squared error. The result of the image registration procedure is specified as a 3×3 transformation matrix $\mathbf{\Omega}_t$ as follows,

$$\mathbf{\Omega}_t = \begin{bmatrix} a & b & 0 \\ c & d & 0 \\ t_x & t_y & 1 \end{bmatrix}$$

where a, b, c, and d jointly specify the rotation operations, and t_x and t_y denote the number of pixels to shift the image in the horizontal and vertical direction, respectively. More specifically, two possible special cases of $\mathbf{\Omega}_t$ are discussed as follows.

Case 1: When $b = c = 0, and\ a = d = 1$, $\mathbf{\Omega}_t$ specifies a registration function with a translation operation only;

Case 2: When a, b, c, and d satisfy $a = d = \cos q\ \ and\ b = -c = \sin q$ where q represents the angle of rotation about the origin of the image, $\mathbf{\Omega}_t$ specifies a registration function with both rotation and translation operations;

2.2.2 Gaussian Process Model

Gaussian Process (GP) modeling technique has an advantage to develop the model with the help of identifying the structure of the covariance matrix of the explanatory variables. This feature makes the GP model more flexible than traditional approaches, which consider only the algebraic structure of the input–output relationship. Therefore, the GP model is able to capture strong nonlinearities and multivariate interactions in a systematic way. Derived from a Bayesian setting, the GP enables to combine and quantify separate sources of uncertainty in a natural way [12-13].

The error term ε_t in Equation (1) is modeled as follows,

$$\varepsilon_t \sim GP\left(\beta_t, K\left((i,j),(i',j')\right) + \sigma_t^2 I\right) \quad (2)$$

where i and j denote the row and column indices of the pixel in the error term matrix ε_t $i = 1,2,3,\dots,I, and\ j = 1,2,3,\dots,J$. β_t represents the mean of the Gaussian process ε_t, whereas σ_t^2 shows the white noise variation of pixels. $K(\cdot,\cdot)$ represents the kernel function used to characterize the covariance between the two different locations, i.e. (i,j) and (i',j'). In Gaussian processes, the covariance function characterizes the correlation (similarity) between neighboring pixels within the ε_t matrix, which obviously have similar response values. In other words, it determines how the response at each pixel is affected by responses at other pixels. The covariance function $K(\cdot,\cdot)$ can be defined by various kernel functions, which can be parameterized in terms of different kernel parameters.

In this paper, Matern 3/2 covariance kernel function is used to characterize the spatial correlation in ε_t's as follows,

$$K\left((i,j),(i',j')|\sigma_l,\sigma_f\right) = \sigma_f^2\left(1+\frac{\sqrt{3}r}{\sigma_l}\right)\exp\left(-\frac{\sqrt{3}r}{\sigma_l}\right) \quad (3)$$

where r is the Euclidean distance between the two pixels (i,j) and (i',j'), i.e., $r = \sqrt{(i-i')^2+(j-j')^2}$, as illustrated in Figure 3; σ_l is the characteristic length scale, and σ_f is the signal standard deviation [14]. It is worth noting that Quasi-Newton optimizer is used for parameter estimation in the GP.

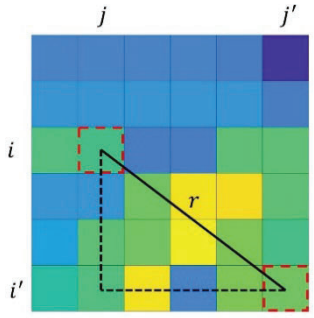

Figure 3: Distance between pixels in a thermal image

2.3.Layer-wise Feature Extraction

There are two groups of features extracted to characterize the thermal image series: one is extracted from the transformation matrix obtained from the registration function, and the other is extracted from the estimated parameters from the GP models to characterize the error matrix.

Image registration related features are extracted from the transformation matrix $\mathbf{\Omega}_t$. Without losing generality, it is assumed that the transformation can be achieved by a sequence of image operations as rotation, and translation, i.e.,

$$\mathbf{\Omega}_t = \begin{bmatrix} a & b & 0 \\ c & d & 0 \\ t_x & t_y & 1 \end{bmatrix} = \mathbf{\Omega}_t^{\mathrm{R}} \times \mathbf{\Omega}_t^{\mathrm{T}}$$

where the rotation and translation parameters can be identified: 1) the rotation angle $q = \tan^{-1}\left(\frac{b}{a}\right)$; 2) the translation in horizontal and vertical directions are t_x and t_y, respectively.

Two features can be extracted from parameter q, t_x and t_y. In order to extract a feature from translation, t_x and t_y are used to calculate the Euclidian distance shifted from the original image and registered image as follows,

$$ED_{l,t} = \sqrt{t_x^2 + t_y^2} \tag{4}$$

In order to modify this variable for layer-wise prediction, the maximum of $ED_{l,t}$'s over the consecutive image pairs of a layer is considered, Therefore, the feature extracted from image registration translation will be presented as

$$F_l^1 = \max_{1 \le t \le T_l - 1} \{ED_{l,t}\} \tag{5}$$

Similarly, the feature to characterize the rotation operation can be calculated as

$$F_l^2 = \max_{1 \le t \le T_l - 1} \{|q_{l,t}|\} \tag{6}$$

The next category of features is extracted by parameters of GP model which are defined as $F_{l,t}^3 = \beta_t$ which is the maximum of β over images of a layer, $F_{l,t}^4 = \sigma_t$ and $F_{l,t}^5 = \sigma_{t,L}$; $F_{l,t}^6 = \sigma_{t,f}$ which are based on variation of pixels, characteristic length scale and the signal standard deviation, respectively. Again the maximum of each feature for a single layer is calculated to obtain the layer-wise features as $F_l^i = \max_{1 \le t \le T_l - 1} \{F_{l,t}^i\}$, where $i = 3, 4, 5, 6$.

It is worth noting that when coaxial thermal monitoring systems are used, the location of the melt pools does not change over time under the normal processing condition. Therefore, Eq. (5) works for all different printing paths. However, Eq. (6) works only when the printing path is unidirectional, where the theoretical rotation angle equals to 0. However, for complicated scanning path, the calculated rotation parameter needs to be compared with the theoretical rotation based on the designed scanning path. As illustrated in Figure 4, the moving direction of laser is changing over the time. In that case, F_l^2 feature is calculated as follows,

$$F_l^2 = \max_{1 \le t \le T_l - 1} \{|q_{l,t} - \Delta\theta_{t,t+1}|\} \tag{7}$$

where $\Delta\theta_{t,t+1}$ represents the theoretical rotation angle between the two consecutive melt pools. An example is shown in Figure 4 in which two melt pools observed in a same layer have different moving directions, where $\Delta\theta_{t,t+1} = \theta_{t+1} - \theta_t$. In other words, Eq. (7) is the general form of Eq. (6). The features from the error term apply to all different scanning paths as all the assignable changes should be incorporated in the registration operation.

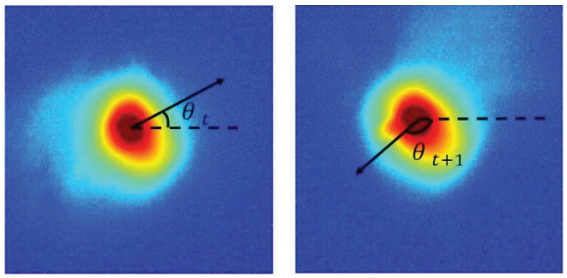

Figure 4: Consecutive thermal images with different moving direction

2.4. Classification: Correlating Layer Signatures to Structural Quality

When structural quality information, such as X-ray CT scanned results, is available. Supervised learning methods can be used to train a classification model. Support Vector Machine (SVM) is considered as a powerful classification technique with a diversity of kernel functions. By finding the best hyperplane that separates all data points of different classes, an SVM classifier can be trained using data labeled with X-ray CT evaluations. More specifically, a layer that contains at least one porosity is labeled as unhealthy, and a porosity-free layer is labeled as healthy. Among SVM classifiers, linear SVM is applied in this paper for simplicity and better interpretability. To achieve more flexibility, more sophisticated kernels such as Gaussian kernel or polynomial kernel can be used [15]. It is worth noting that various other machine learning algorithms can also be applied to this problem. Comparing classification performance of different machine learning schemes is out of the scope of this paper.

3. Case Study

The performance of the proposed methodology is validated using a direct laser deposition process. A thin wall of 60 layers in total was fabricated using Ti-6AL-4V. During the fabrication, the thermal images of the melt pools related to different locations on the thin wall are captured by a pyrometer camera. The number of thermal images captured using co-axial pyrometer camera is 1564 with each represented by a 480 × 752 matrix of pixels. The process setup parameters are summarized in Table 1 [5]. After the build was completed, the porosity structure inside the build was identified using an X-ray CT scan (Skyscan 1172). The X-ray examination indicated that 26 layers out of 60 layers of the thin wall include at least one porosity. Figure 5 illustrates a melt pool image series within a layer containing a porosity related to an unhealthy melt pool at t+17. It is worth noting that minimum size for a pore is $0.05\mu m$.

Table 1: LENS process design parameters for the thin wall.

Scan speed	12.70 mm/s	Starting offset from substrate	130.391mm
Powder feed rate	0.060 g/s	Determination of layer thickness	0.508 mm
Determination of hatch spacing	0.508 mm	Nozzle diameter	0.889 mm
Power	300 W	Substrate (stainless steel)	3.175 mm

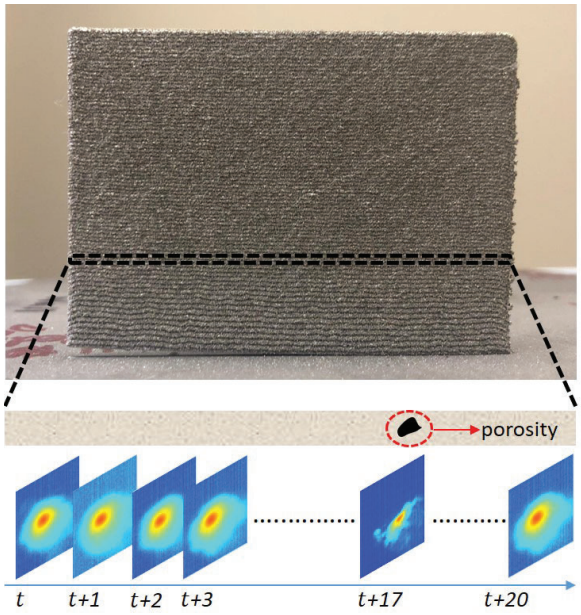

Figure 5: The image of a thin wall containing one pore in an unhealthy layer

For image registration, due to the printing path design was unidirectional, the orientation of the melt pool image should not change over time. Therefore, only translation operation is estimated in the transformation matrix $\mathbf{\Omega}_t$. Fabricating a thin wall, the melt pool only shifts from image to image and the melt pool is not subjected to rotation. Regarding that the only transformation that can be applicable is translation, the feature extracted from translation are the only feature extracted from the image registration process. The error term ε_t's were modeled using Gaussian process models, and the layer-wise features were obtained by calculating the maximum values for each feature.

Leave-one-out validation was used to test the effectiveness of the proposed method. Table 2 illustrates the confusion matrix after implementing the aforementioned model. Four layers out of 60 layers (6.67% of the total layers) are misclassified, in which two misclassifications for healthy and two for unhealthy. The recall, precision, and *F*-score were considered as three measures to define the accuracy of the model and calculated as follows:

$$Recall = \frac{TP}{TP + FN}$$

$$Precision = \frac{TP}{TP + FP}$$

$$F - score = 2 \times \frac{Precision \times Recall}{Precision + Recall}$$

where *F*-score is the harmonic mean of precision and recall. TP shows true positive layers which are healthy and predicted accurately as unhealthy. TN stands for true negative that illustrated the items that are accurately predicted as healthy. On the other hand, FN defines inaccurate prediction that are actually unhealthy, while FP shows inaccurate prediction that are actually healthy.

Table 2: Confusion Matrix for Leave-one-out Cross Validation

		Predicted	
		Healthy	Unhealthy
Actual	Healthy	32	2
	Unhealthy	2	24

The results indicate that the recall and precision of leave-one-out cross validation are 0.9231 and 0.9231, respectively, and consequently, the *F*-score is also 0.9231. This indicates that the classification model accuracy is reasonably high and can be used for layer-wise anomaly detection. One of the possible reasons for misclassification is the discrete data sampling for thermal history fails to capture the thermal image when the anomaly occurs. Consequently, some information will be missed. In addition, the X-ray CT scans may be subject to noise and error as well. Moreover, the proposed anomaly detection method does not consider effects of re-melting, which can potentially correct some of the porosities generated in the previous layer.

4. Conclusion

Lack of repeatability in the additively fabricated parts is one of the major challenges that hinders broader industrial applications of additive manufacturing processes. Possible build quality issues, such as internal porosity, deformation, and cracking, can lead to significantly compromised mechanical properties. Comprehensive studies including data-driven methods have been focused on local characterization for anomaly detection based on single thermal images. A layer-wise thermal image modeling framework can take into account the complex spatio-temporal relationship within the image series, which can potential achieve improved anomaly detection results. In this paper, the layer-wise thermal images are formulated as an image series, and an image-based autoregressive (AR) model has been proposed based on the registration function between consecutively observed thermal images. Multiple features are extracted from the AR model for each consecutive pair of images, and layer-wise features are extracted subsequently. Support Vector Machine method is used for anomaly detection based on the extracted layer-wise features. A case study based on a thin wall fabrication using a DLD process is used to validate the proposed methodology. The classification accuracy of the proposed method is reasonably high which makes the model capable of predicting defects. For future works, the represented model can be applied to the thermal image analysis of AM parts with more complicated geometry.

5. Acknowledgment

Research was sponsored by the Army Research Laboratory and was accomplished under Cooperative Agreement Number W911NF-15-2-0025. The views and conclusions contained in this document is those of the authors and should not be interpreted as representing the official policies, either expressed or implied, of the Army Research Laboratory or the U.S. Government. The U.S. Government is authorized to reproduce and distribute reprints for Government purposes notwithstanding any copyright notation herein.

6. References

[1] M. Grasso and B. M. Colosimo, “Process defects and *in situ* monitoring methods in metal powder bed fusion: a review,” Measurement Science Technology, vol. 28, no. 4, p. 44005, Apr. 2017.

[2] M. Matsumoto, M. Shiomi, K. Osakada, and F. Abe, “Finite element analysis of single layer forming on metallic powder bed in rapid prototyping by selective laser processing,” International Journal of Machine Tools and Manufacture, vol. 42, no. 1, pp. 61–67, 2002.

[3] R. Martukanitz *et al.*, “Toward an integrated computational system for describing the additive manufacturing process for metallic materials,” Additive Manufacturing, vol. 1, pp. 52–63, 2014.

[4] M. Khanzadeh, S. Chowdhury, M. Marufuzzaman, and M. A. Tschopp, “Porosity prediction: Supervised-learning of thermal history for direct laser deposition Data analytics and statistical learning in Additive Manufacturing View project Deformation in HCP materials View project,” *Artic. J. Manuf. Syst.*, 2018.

[5] M. Khanzadeh, S. Chowdhury, M. A. Tschopp, H. R. Doude, M. Marufuzzaman, and L. Bian, “In-situ monitoring of melt pool images for porosity prediction in directed energy deposition processes,” IISE Transactions, vol. 5854, pp. 1–19, 2018.

[6] J. Matoušek, *Lectures on discrete geometry*, vol. 212. Springer New York, 2002.

[7] J. Liu *et al.*, “Layer-Wise Spatial Modeling of Porosity in Additive Manufacturing Real-time process monitoring for advanced manufacturing View project Sensing and Data Analytics for Additive Manufacturing View project Layer-wise Spatial Modeling of Porosity in Additive M,” vol. 10, no. May, 2018.

[8] Caltanissetta, F., Grasso, M., Petro, S. and Colosimo, B.M., 2018. Characterization of in-situ measurements based on layerwise imaging in laser powder bed fusion. Additive Manufacturing, 24, pp.183-199.

[9] Imani, F., Gaikwad, A., Montazeri, M., Rao, P., Yang, H. and Reutzel, E., 2018. Process mapping and in-process monitoring of porosity in laser powder bed fusion using layerwise optical imaging. Journal of Manufacturing Science and Engineering, 140(10), p.101009.

[10] S. M. Thompson, L. Bian, N. Shamsaei, and A. Yadollahi, “An overview of Direct Laser Deposition for additive manufacturing; Part I: Transport phenomena, modeling and diagnostics,” Additive Manufacturing, vol. 8, pp. 36–62, 2015.

[11] Damas, Sergio, Oscar Cordón, and Jose Santamaría. "Medical image registration using evolutionary computation: An experimental survey." IEEE Computational Intelligence Magazine 6.4 (2011): 26-42.

[12] C.E. Rasmussen, C.K. Williams, Gaussian Processes for Machine Learning, MIT Press, Cambridge, MA, 2006.

[13] C.J. Paciorek, M.J. Schervish, Nonstationary covariance functions for Gaussian process regression, in: Advances in Neural Information Processing Systems 16: Proceedings of the 2003 Conference, Bradford Book, British Columbia, Canada, 2004, p. 273.

[14] Rasmussen, C. E. and C. K. I. Williams. *Gaussian Processes for Machine Learning.* MIT Press. Cambridge, Massachusetts, 2006.

[15] Cristianini, N. and Shawe-Taylor, J., 2000. An introduction to support vector machines and other kernel-based learning methods. Cambridge University Press.